Electronic Supplementary Material (ESI) for Energy & Environmental Science.

Supporting information for: Modeling the electrical double layer to understand the reaction environment in a CO_2 electrocatalytic system

Divya Bohra,[†] Jehanzeb H. Chaudhry,[‡] Thomas Burdyny,[†] Evgeny A. Pidko,[¶] and Wilson A. Smith[*,†]

†*Materials for Energy Conversion and Storage (MECS), Department of Chemical Engineering, Delft University of Technology, 2629 HZ Delft, The Netherlands*

‡*Department of Mathematics and Statistics, University of New Mexico, 310 SMLC, Albuquerque, NM, 87131, USA.*

¶*Inorganic Systems Engineering (ISE), Department of Chemical Engineering, Delft University of Technology, 2629 HZ Delft, The Netherlands*

E-mail: W.Smith@tudelft.nl

Model details

Simulation domain

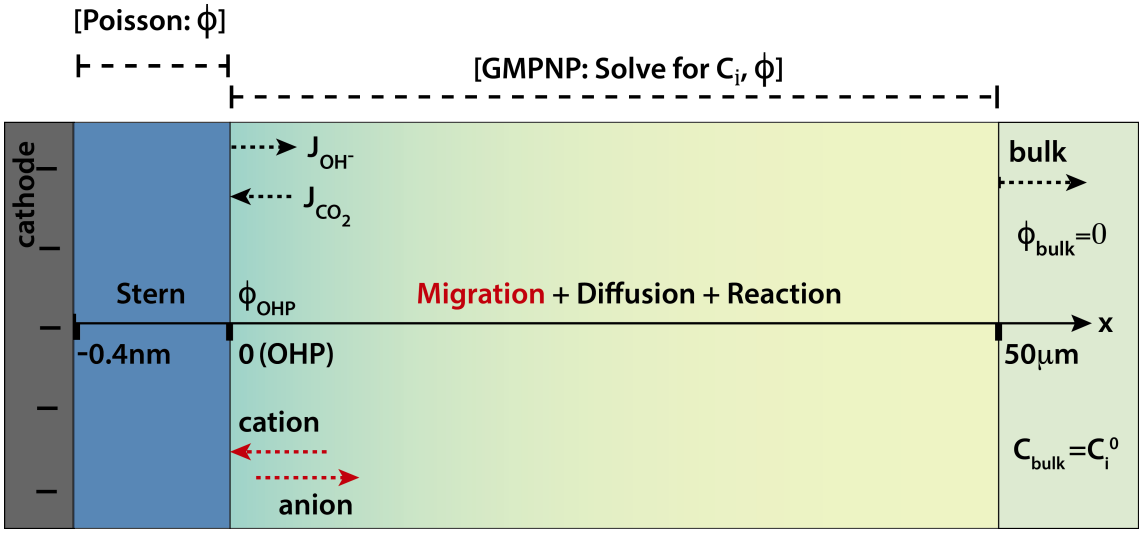

Figure S1

Calculating bulk concentrations

We assume Henry's law to be valid for CO_2 gas and calculate its concentration in water using equation (1). We assume the fugacity of CO_2 to be 1 bar.

$$C^0_{CO2,aq} = K^0_H C_{CO2,g} \tag{1}$$

where K^0_H is Henry's constant and is given as a function of temperature T by equation (2).[S1] The temperature is assumed to be 298.15 K for our calculations.

$$\ln K^0_H = 93.4517 * \left(\frac{100}{T}\right) - 60.2409 + 23.3585 * \ln\left(\frac{T}{100}\right) \tag{2}$$

The saturated concentration of CO_2 in an electrolyte ($C_{CO2,aq}$) with 0.1 M $KHCO_3$ is then given by equation (3).[S2]

$$\log\left(\frac{C^0_{CO2,aq}}{C_{CO2,aq}}\right) = K_S C_S \tag{3}$$

where C_S is the molar concentration of the electrolyte (0.1) and K_S is the Sechenov's constant and can be estimated using parameters h_i for species i. Values of h for all species can be found in the Parameters section.

$$K_S = \sum(h_{CO2} + h_{ion}) \tag{4}$$

$$h_{CO2} = h^0_{CO2} + h^T_{CO2}(T - 298.15) \tag{5}$$

In order to calculate the concentration of solution species in the bulk electrolyte, the Sechenov equation (3) is used to estimate the saturated concentration of CO_2 in a 0.1 M $KHCO_3$ electrolyte. The estimated CO_2 concentration is then used to solve the rate equations (6) to (10) (corresponding to equations (6), (7) and (8) in the main text) till steady state is reached.

$$R_{H^+} = \frac{\partial C_{H^+}}{\partial t} = -k_{w2} C_{H^+} C_{OH^-} + k_{w1} \tag{6}$$

$$R_{OH^-} = \frac{\partial C_{OH^-}}{\partial t} = -k_{w2} C_{H^+} C_{OH^-} - k_{a1} C_{OH^-} C_{HCO_3^-} - k_{b1} C_{CO_2} C_{OH^-} + k_{w1} + k_{a2} C_{CO_3^{2-}} + k_{b2} C_{HCO_3^-} \tag{7}$$

$$R_{HCO_3^-} = \frac{\partial C_{HCO_3^-}}{\partial t} = -k_{a1} C_{OH^-} C_{HCO_3^-} - k_{b2} C_{HCO_3^-} + k_{a2} C_{CO_3^{2-}} + k_{b1} C_{CO_2} C_{OH^-} \tag{8}$$

$$R_{CO_3^{2-}} = \frac{\partial C_{CO_3^{2-}}}{\partial t} = -k_{a2} C_{CO_3^{2-}} + k_{a1} C_{OH^-} C_{HCO_3^-} \tag{9}$$

$$R_{CO_2} = \frac{\partial C_{CO_2}}{\partial t} = -k_{b1} C_{CO_2} C_{OH^-} + k_{b2} C_{HCO_3^-} \tag{10}$$

The resulting bulk species concentrations for a 0.1 M $KHCO_3$ electrolyte saturated with CO_2 at 1 bar and room temperature are (in mM): $C^0_{CO2} = 34.061$, $C^0_{CO_3^{2-}} = 0.039$, $C^0_{H^+} = 0.00014$, $C^0_{HCO_3^-} = 99.920$, $C^0_{K^+} = 100.0$, $C^0_{OH^-} = 7.1\text{e-}05$, pH = 6.853.

Deviation from equilibrium

Equilibrium constants for the reactions (6), (7) and (8) in the main text are defined as:

$$Keq_w = \frac{k_{w1}}{k_{w2}} \quad and \quad Keq_a = \frac{k_{a1}}{k_{a2}} \quad and \quad Keq_b = \frac{k_{b1}}{k_{b2}}$$

The deviation of the homogeneous reactions from their equilibrium is then defined as:

$$dev_{water-dissociation} = 1 - \frac{[\mathrm{H^+}][\mathrm{OH^-}]}{Keq_w} \tag{11}$$

$$dev_{bicarbonate-carbonate} = 1 - \frac{[\mathrm{CO_3^{2-}}]}{[\mathrm{HCO_3^-}][\mathrm{OH^-}]Keq_a} \tag{12}$$

$$dev_{CO2-bicarbonate} = 1 - \frac{[\mathrm{HCO_3^-}]}{[\mathrm{CO_2}][\mathrm{OH^-}]Keq_b} \tag{13}$$

Limiting H^+ current case

In the limiting H^+ current case, a proton consumption current is added to the overall current such that only <10% of the bulk proton concentration is allowed to be present at the OHP at steady state. The H^+ at the OHP is consumed in the heterogeneous reactions:

$$2\,\mathrm{H^+} + 2\,\mathrm{e^-} \rightleftharpoons \mathrm{H_2(g)} \tag{14}$$

$$\mathrm{CO_2(aq)} + 2\,\mathrm{H^+} + 2\,\mathrm{e^-} \rightleftharpoons \mathrm{CO(g)} + \mathrm{H_2O} \tag{15}$$

The OH^- and H^+ flux at the OHP (x=0) then becomes:

$$\vec{J}_{OH^-}|_{x=0,t} = -\frac{j_{tot}}{F} \times (1 - j_{H^+frac}) \tag{16}$$

$$\vec{J}_{H^+}|_{x=0,t} = \frac{j_{tot}}{F} \times j_{H^+frac} \tag{17}$$

where j_{H^+frac} is the fraction of the total current density due to H^+ consumption. The CO_2 flux remains the same as in equation (4) in the main text.

Scaling the GMPNP equations

We scale the GMPNP equations (9), (10) and (11) in the main text and write them using dimensionless variables as follows:

$$\frac{1}{\Lambda_D}\frac{\partial \tilde{C}_i}{\partial \tau} = \nabla \cdot \left(\nabla \tilde{C}_i + \tilde{C}_i z_i \nabla \Phi + \tilde{C}_i \left(\frac{\sum_{i=1}^{n} \upsilon_i \nabla \tilde{C}_i}{1 - \sum_{i=1}^{n-1} \upsilon_i \tilde{C}_i} \right) \right) + \sum_p \vartheta_{ip} R_i \tag{18}$$

$$\nabla \cdot (\varepsilon_r \nabla \Phi) = -q \sum_{i=1}^{n} z_i \tilde{C}_i \tag{19}$$

$$L_{debye} = \sqrt{\frac{\varepsilon_0 \varepsilon_r^0 k_B T}{2 e_0^2 C_{elec} N_A}} \tag{20}$$

$$\nabla = \frac{\partial}{\partial \tilde{x}}, \Lambda_D = \frac{L_{debye}}{L_n}, \tilde{x} = \frac{x}{L_n}, \tau = \frac{t D_i}{L_{debye} L_n}, \tilde{C}_i = \frac{C_i}{C_i^0},$$

$$\Phi = \frac{\phi F}{RT}, \vartheta_{ip} = \frac{L_n^2}{D_i C_i^0}, \upsilon_i = a_i^3 N_A C_i^0, q = \frac{(F L_n)^2 C_i^0}{\varepsilon_0 RT}$$

where L_n is the system length which is assumed to be 50 μm, L_{debye} is the Debye length as defined by equation (20), C_{elec} is the bulk concentration of the electrolyte, e_0 is the fundamental charge of electron and C_i^0 is the bulk concentration of species i. The equations (18) and (19) are solved simultaneously with the appropriate initial and boundary conditions to obtain the species concentration and potential profiles at steady state.

Reaction-Diffusion and PNP system of equations

Reaction-diffusion model

In the reaction-diffusion model, the flux term in the mass balance equation only contains the diffusion mass transport term and excludes the migration and volume correction terms as given below.

$$\frac{\partial C_i}{\partial t} = -\nabla \cdot \vec{J}_i + \sum_p R_i \tag{21}$$

$$\vec{J}_i = -D_i \nabla C_i \tag{22}$$

PNP equations

The Poisson-Nernst-Planck (PNP) equations solve the dynamics of the mass transport of solution species including the effects of diffusion, reaction as well as migration such that equations (23) and (25) are solved simultaneously. However, dilute solution theory is used and the equations are valid for point species.

$$\frac{\partial C_i}{\partial t} = -\nabla \cdot \vec{J}_i + \sum_p R_i \tag{23}$$

$$\vec{J}_i = -D_i \nabla C_i - \frac{D_i C_i z_i F}{RT} \nabla \phi \tag{24}$$

$$\nabla \cdot (\varepsilon_0 \varepsilon_r \nabla \phi) = -F \sum_{i=1}^{n} z_i C_i \tag{25}$$

Equation (12) in the main text is assumed to hold for the relative permittivity (ε_r). For both the reaction-diffusion and PNP systems, R_i are as given in equations (6) to (10) and the boundary conditions used for the species concentrations are the same as that for the GMPNP system of equations.

SUPG Stabilization of the PNP system

A Streamlined Upwind Petrov-Galerkin (SUPG) stabilization was used for the PNP equations to be able to resolve the steady-state concentration and potential profiles at practically relevant applied voltages for a system of size 50 μm.[S3–S6]

$$\vec{b_i} = -z_i \nabla \Phi \tag{26}$$

$$\sigma_{i\iota} = \sigma_{i\iota}^{0} \times Pe_{i\iota} \tag{27}$$

where

$$\sigma_{i\iota}^{0} = \frac{h_{\iota}}{2|z_i|\|\nabla\Phi\|_2} \tag{28}$$

and

$$Pe_{i\iota} = \begin{cases} \frac{h_{\iota}|z_i|\|\nabla\Phi\|_2}{2} & \text{if } Pe_{i\iota} \leq 1 \\ 1 & \text{if } Pe_{i\iota} > 1 \end{cases} \tag{29}$$

$\vec{b_i}$ is the flow field due to migration which is the equivalent dimensionless velocity term in equation (23) and (24). $\sigma_{i\iota}$ and $Pe_{i\iota}$ are the stability parameter for the SUPG term and the Péclet number for species i for element ι of the mesh, respectively.

The test function of the SUPG stabilization term in the Galerkin form is then given by:

$$\nu_{i\iota}^{SUPG} = \sigma_{i\iota}\vec{b_i}\cdot\nabla v_i = \begin{cases} -\frac{h_{\iota}^2 z_i}{4}\nabla\Phi\cdot\nabla v_i & \text{if } Pe_{i\iota} \leq 1 \\ -\frac{h_{\iota} z_i}{2|z_i|\|\nabla\Phi\|_2}\nabla\Phi\cdot\nabla v_i & \text{if } Pe_{i\iota} > 1 \end{cases} \tag{30}$$

The SUPG stabilization term in its weak-form for the Nernst Planck equations (NP) is given by multiplying the test function as given by equation (30) to the residual of the NP. The overall stabilized NP equation is then given by equation (31).

$$\int_{\Omega}\left(\left(\frac{\tilde{C_i}^{n+1} - \tilde{C_i}^{n}}{\Delta\tau \times \Lambda_D}\right) - \nabla\cdot\left(\nabla\tilde{C_i} + \tilde{C_i} z_i \nabla\Phi\right) - \sum_{p}\vartheta_{ip}R_i\right) v_i \partial x +$$

$$\sum_{\iota\epsilon I}\int_{\iota}\left(\left(\frac{\tilde{C_i}^{n+1} - \tilde{C_i}^{n}}{\Delta\tau \times \Lambda_D}\right) - \nabla\cdot\left(\nabla\tilde{C_i} + \tilde{C_i} z_i \nabla\Phi\right) - \sum_{p}\vartheta_{ip}R_i\right) \nu_{i\iota}^{SUPG}\partial x \tag{31}$$

where the first integral term in equation (31) is nothing but the residual of the scaled PNP equation multiplied by the test function v_i and integrated over the entire finite element domain Ω. The second term in equation (31) is the stabilization term which is a summation

of the residual multiplied by the test function for SUPG (equation (30)) integrated over each element in the mesh.

The first term in equation (31) is integrated by parts to derive the weak form as is common in finite element mothods. We drop the higher order differential terms in the SUPG stabilization (second term in equation (31)) since the basis functions used for the finite element solver as piece-wise linear. The final form of the stabilized scaled NP equation is given by (32).

$$\int_{\Omega}\left(\left(\frac{\tilde{C_i}^{n+1}-\tilde{C_i}^{n}}{\Delta\tau\times\Lambda_D}\right)-\nabla\cdot\left(\nabla\tilde{C_i}+\tilde{C_i}z_i\nabla\Phi\right)-\sum_{p}\vartheta_{ip}R_i\right)v_i\partial x+$$

$$\sum_{\iota\epsilon I}\int_{\iota}\left(\left(\frac{\tilde{C_i}^{n+1}-\tilde{C_i}^{n}}{\Delta\tau\times\Lambda_D}\right)-z_i\nabla\tilde{C_i}\cdot\nabla\Phi-\sum_{p}\vartheta_{ip}R_i\right)\nu_{i\iota}^{SUPG}\partial x \tag{32}$$

Note that although the Poisson equation is solved simultaneously with the NP equation, it does not feature in the stabilization implemented. Equation (32) is simultaneously solved with the Poisson equation with the initial and boundary conditions mentioned in the main text.

PZC values for Ag

Potential at the point of zero charge in V vs SHE at pH=7:[S7]

Surface	Value
Ag-pc	-0.70
Ag(111)	-0.450
Ag(110)	-0.735
Ag(100)	-0.616

Parameters

Rate-constants:

Constant	Value	Units	Reference
kw1	2.4e-2	molm-3s-1	S8–S10
kw2	2.4e+6	mol-1m3s-1	S8–S10
ka1	6.0e+6	mol-1m3s-1	S11
ka2	1.07e+6	s-1	S11
kb1	2.23	mol-1m3s-1	S11
kb2	5.23e-5	s-1	S11

Diffusion-coefficients in $m^2 s^{-1}$:

Constant	Value	Reference
D_{H+}	9.311e-9	S8,S9
D_{OH-}	5.273e-9	S8,S9
D_{CO2}	1.91e-9	S8,S9
D_{HCO3-}	1.185e-9	S8,S9
D_{CO32-}	0.923e-9	S8,S9
D_{K+}	1.957e-9	S12
D_{Na+}	1.334e-9	S12
D_{Li+}	1.029e-9	S12
D_{Cs+}	2.06e-9	S12

Solvation sizes in m:[S13]

Constant	Value
a_{H+}	0.56e-9
a_{OH-}	0.6e-9
a^{**}_{CO2}	0.23e-9
a^{*}_{HCO3-}	0.8e-9
a_{CO32-}	0.788e-9
a_{K+}	0.662e-9
a_{Na+}	0.716e-9
a_{Li+}	0.764e-9
a_{Cs+}	0.658e-9

* The solvated size of HCO_3^- is assumed to be similar to CO_3^{2-} due to unavailability of a reliable value in literature. ** The solvated size of CO_2 is assumed to be twice the C=O bond distance.

Parameters used to estimate Sechenov's constant in $m^3 kmol^{-1}$:[S2]

Constant	Value
h_{K+}	0.0922
h_{OH-}	0.0839
h_{HCO3-}	0.0967
h_{CO32-}	0.1423
h^{0}_{CO2}	-0.0172
h^{T}_{CO2}	-0.000338

Hydration numbers for cations used in equation (12) in the main text:[S14,S15]

Constant	Value
w_{K+}	4
w_{Li+}	5
w_{Na+}	5
w_{Cs+}	3
w_{H+}	10

Supplimentary Results

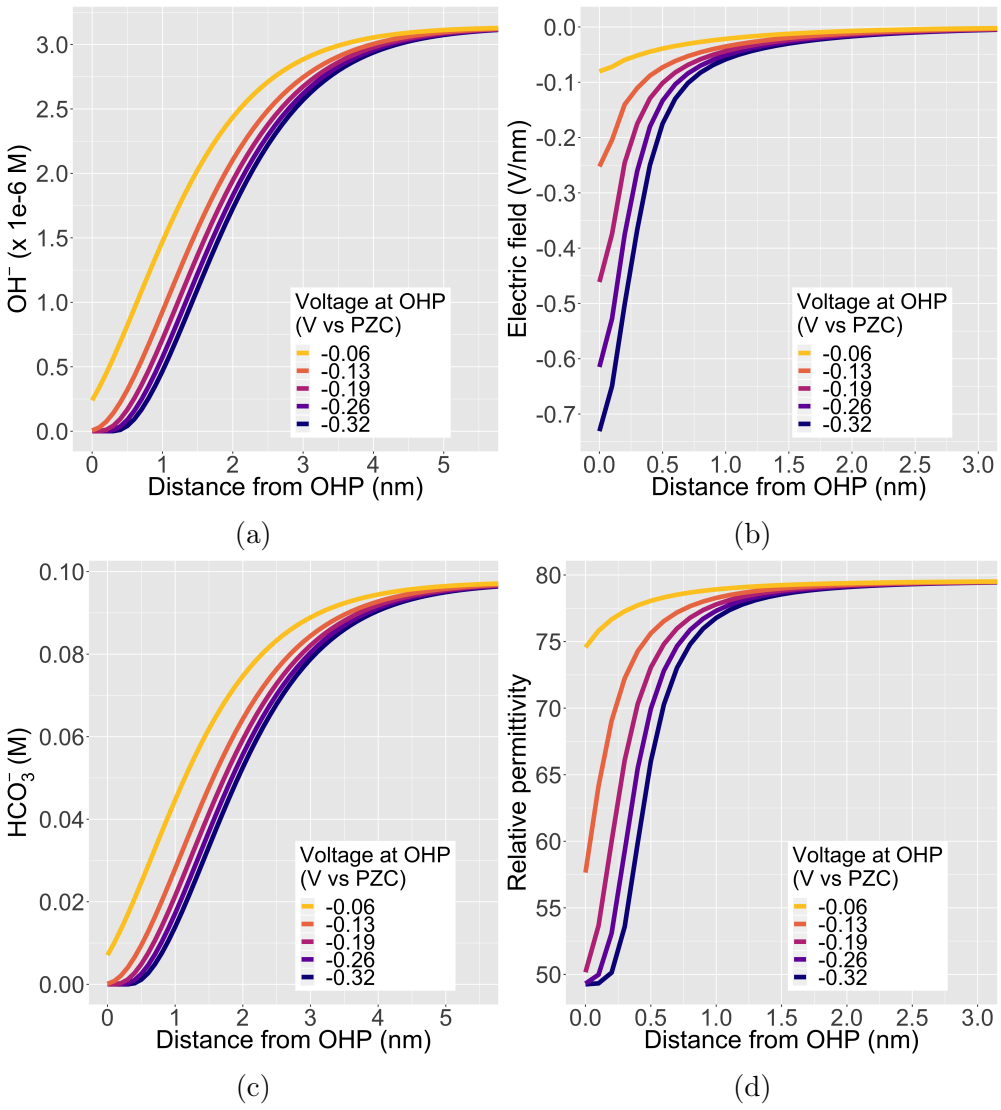

Figure S2: The electrical double layer (EDL) facing a planar CO_2ER catalyst for a 0.1 M $KHCO_3$ electrolyte solution saturated with CO_2. The above results are derived for a total current density of 1 mA/cm^2 and a CO Faradaic efficiency of 0.8. PZC stands for the potential of point of zero charge of the planar catalyst surface and x=0 is the OHP.

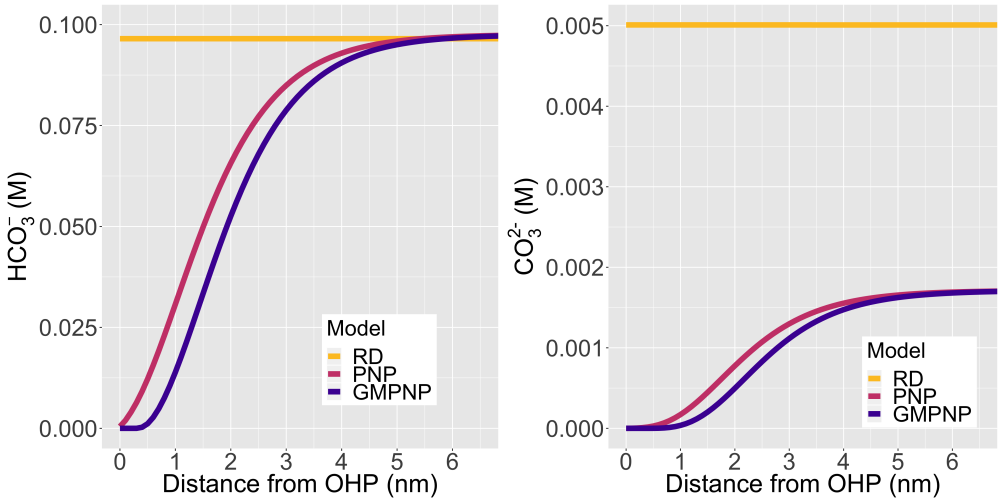

(a) (b)

Figure S3: Comparison between results obtained from reaction-diffusion (RD) model, a Poisson-Nernst-Planck (PNP) model and a generalized modified PNP (GMPNP) model for the EDL region. x=0 is located at the OHP. All results have been derived for a total current density of 1 mA/cm^2 and a CO Faradaic efficiency of 0.8. The PNP and GMPNP results are for a voltage of -0.32 V vs PZC at the OHP.

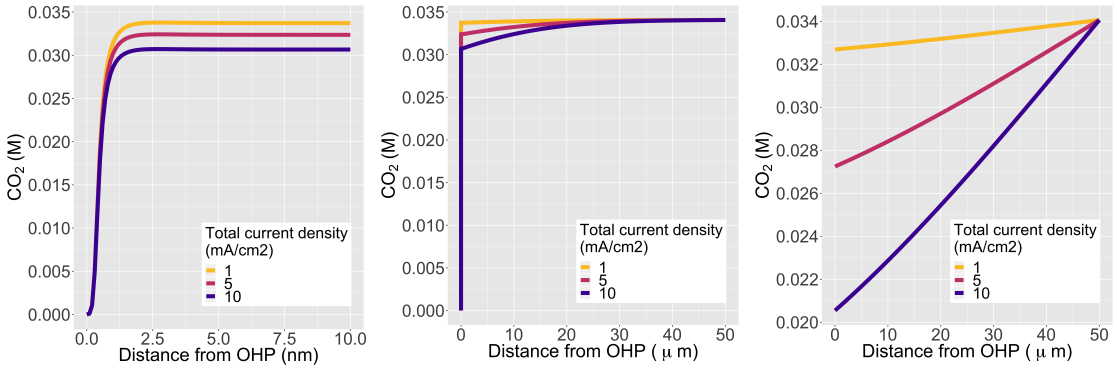

(a) GMPNP: EDL (b) GMPNP: Full domain (c) RD: Full domain

Figure S4: Influence of total current density on CO_2 concentration derived using the GMPNP model. Figure (a) shows the profiles for a region of 10 nm from the OHP whereas Figure (b) shows the profiles for the entire Nernst layer extending to 50 μm. Figure (c) shows results obtained using reaction-diffusion (RD) model for the purpose of comparison. All results are calculated for a CO Faradaic efficiency of 0.8 and the GMPNP results are for a potential of -0.32 V vs PZC at the OHP.

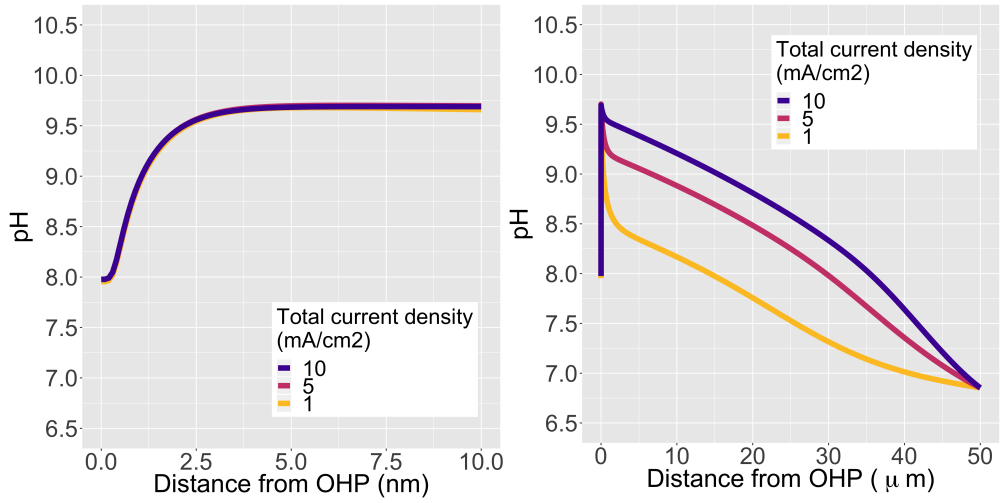

(a) (b)

Figure S5: Influence of total current density on pH derived using the GMPNP model for the limiting H^+ current case where no more than 10% of the bulk proton concentration is allowed to be present at the OHP (x=0). Figure (a) shows the profiles for a region of 10 nm from the OHP whereas Figure (b) shows the profiles for the entire Nernst layer extending to 50 μm. All results are calculated for a CO Faradaic efficiency of 0.8 and for a potential of -0.32 V vs PZC at the OHP.

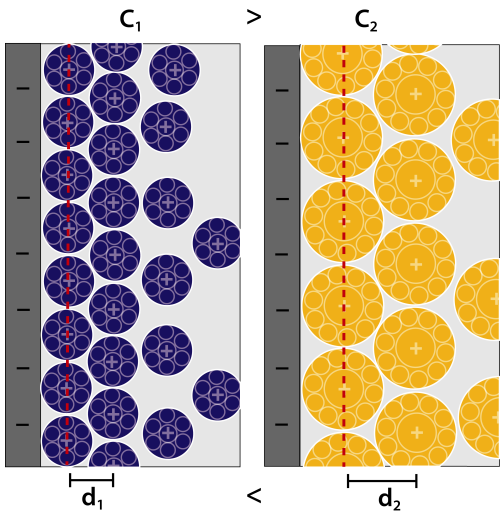

Figure S6: Illustration of the qualitative difference in the concentrations and potential screening lengths of a small solvated cation vs. a large solvated cation acting as counter-ions in the EDL. The red dashed line represents the OHP. C_i and d_i are concentration at the OHP at the steric limit and the width of the condensed region of the EDL, respectively for cation i.

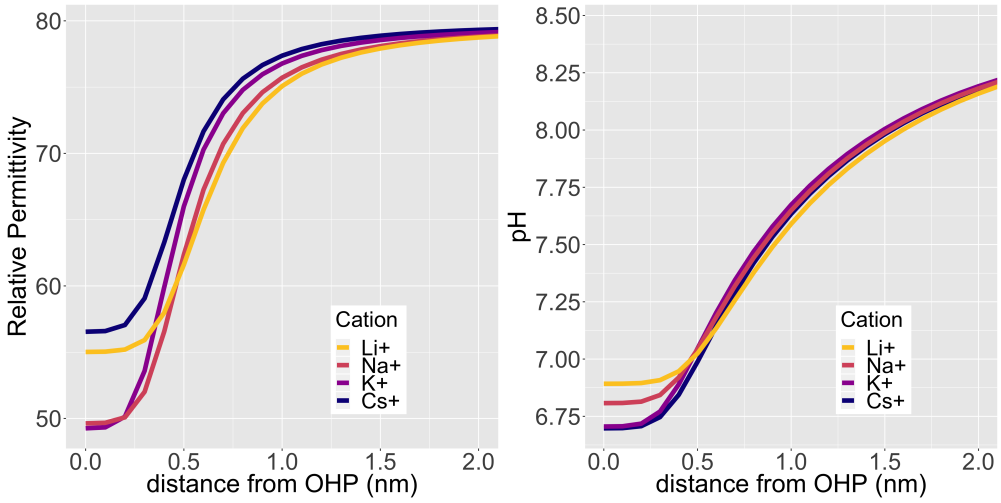

(a) (b)

Figure S7: Effect of cation size on the relative permittivity and pH of the EDL. Calculations are performed for a potential of -0.32 V vs PZC at the OHP for a total current density of 1 mA/cm^2 and a CO Faradaic efficiency of 0.8.

References

(S1) Hansson, L.; Fabry, V. J.; Gattuso, J.-P.; Riebesell, U. *Guide to best practices for ocean acidification research and data reporting*; 2010.

(S2) Weisenberger, S.; Schumpe, A. *AIChE Journal* **1996**, *42*, 298–300.

(S3) Chaudhry, J. H.; Comer, J.; Aksimentiev, A.; Olson, L. N. *Communications in computational physics* **2014**, *15*, 10.4208/cicp.101112.100413a.

(S4) Bochev, P. B.; Gunzburger, M. D.; Shadid, J. N. *Computer Methods in Applied Mechanics and Engineering* **2004**, *193*, 2301 – 2323.

(S5) Hughes, T. J.; Franca, L. P.; Hulbert, G. M. *Computer Methods in Applied Mechanics and Engineering* **1989**, *73*, 173 – 189.

(S6) Franca, L. P.; Frey, S. L.; Hughes, T. J. *Computer Methods in Applied Mechanics and Engineering* **1992**, *95*, 253 – 276.

(S7) Trasatti, S.; Lust, E. In *Modern Aspects of Electrochemistry*; White, R. E., Bockris, J. O., Conway, B. E., Eds.; Springer US: Boston, MA, 1999; pp 1–215.

(S8) Singh, M. R.; Goodpaster, J. D.; Weber, A. Z.; Head-Gordon, M.; Bell, A. T. *Proceedings of the National Academy of Sciences* **2017**, *114*, E8812–E8821.

(S9) Singh, M. R.; Clark, E. L.; Bell, A. T. *Phys. Chem. Chem. Phys.* **2015**, *17*, 18924–18936.

(S10) Atkins, P.; de Paula, J.; Keeler, J. *Atkins' Physical Chemistry*, 11th ed.; Oxford University Press, 2017.

(S11) Burdyny, T.; Graham, P. J.; Pang, Y.; Dinh, C.-T.; Liu, M.; Sargent, E. H.; Sinton, D. *ACS Sustainable Chemistry & Engineering* **2017**, *5*, 4031–4040.

(S12) Rumble, J., Ed. *CRC Handbook of Chemistry and Physics*, 100th ed.; CRC Press, 2019.

(S13) Nightingale, E. R. *The Journal of Physical Chemistry* **1959**, *63*, 1381–1387.

(S14) Bockris, J. O.; Reddy, A. K. *Volume 1: Modern Electrochemistry*, 2nd ed.; Springer US, 1998.

(S15) Bockris, J. O.; Saluja, P. P. S. *The Journal of Physical Chemistry* **1972**, *76*, 2140–2151.